
Since January 2020 Elsevier has created a COVID-19 resource centre with free information in English and Mandarin on the novel coronavirus COVID-19. The COVID-19 resource centre is hosted on Elsevier Connect, the company's public news and information website.

Elsevier hereby grants permission to make all its COVID-19-related research that is available on the COVID-19 resource centre - including this research content - immediately available in PubMed Central and other publicly funded repositories, such as the WHO COVID database with rights for unrestricted research re-use and analyses in any form or by any means with acknowledgement of the original source. These permissions are granted for free by Elsevier for as long as the COVID-19 resource centre remains active.

Available online at www.sciencedirect.com
ScienceDirect
Virology 361 (2007) 18–26
VIROLOGY
www.elsevier.com/locate/yviro

Rapid Communication

# Group 2 coronaviruses prevent immediate early interferon induction by protection of viral RNA from host cell recognition

Gijs A. Versteeg, Peter J. Bredenbeek, Sjoerd H.E. van den Worm, Willy J.M. Spaan *

*Molecular Virology Laboratory, Department of Medical Microbiology, Center of Infectious Diseases, Leiden University Medical Center, LUMC E4-P, P.O. Box 9600, 2300 RC Leiden, The Netherlands*

Received 8 December 2006; returned to author for revision 4 January 2007; accepted 18 January 2007
Available online 21 February 2007

**Abstract**

Many viruses encode antagonists to prevent interferon (IFN) induction. Infection of fibroblasts with the murine hepatitis coronavirus (MHV) and SARS-coronavirus (SARS-CoV) did not result in nuclear translocation of interferon-regulatory factor 3 (IRF3), a key transcription factor involved in IFN induction, and induction of IFN mRNA transcription. Furthermore, MHV and SARS-CoV infection could not prevent IFN induction by poly (I:C) or Sendai virus, suggesting that these CoVs do not inactivate IRF3-mediated transcription regulation, but apparently prevent detection of replicative RNA by cellular sensory molecules. Our data indicate that shielding of viral RNA to host cell sensors might be the main general mechanism for coronaviruses to prevent IFN induction.
© 2007 Elsevier Inc. All rights reserved.

*Keywords:* Coronavirus; Murine hepatitis virus; MHV; SARS; SARS-CoV; Interferon; IFN; Antagonist; Poly (I:C); Sendai virus

## Introduction

Type 1 interferons (IFN) are soluble cytokines that mediate an anti-viral state during a wide variety of infections. Their expression is mainly regulated at the level of transcription (Haller et al., 2006). Virus infections activate signaling pathways that eventually result in the production of IFN-β and IFN-α4 (immediate early IFNs). Molecular pattern recognition receptors, such as toll-like receptors (TLRs), are mainly expressed by specialized cells and can be triggered to initiate IFN production. Non-specialized cells like fibroblasts do not express these TLRs. For the induction of IFN-mediated innate immunity, these cells are dependent on the cytoplasmic RNA helicases retinoic acid-inducible gene I (RIG-I) and melanoma differentiation-associated gene 5 (MDA-5) (Haller et al., 2006). The helicases recognize viral RNA and subsequently activate the IFN-mediated innate immune response. RIG-I recognizes RNA with unprotected 5′-triphosphates and is activated upon infection of cells with influenza virus, flaviviruses and paramyxoviruses, whereas MDA-5 induces IFN production in response to double-stranded RNA (dsRNA) such as during picornavirus infection or transfection with poly (I:C) (Hornung et al., 2006; Kato et al., 2006; Pichlmair et al., 2006). Interferon regulatory factors (IRF), such as IRF3, are the key switches for the transcription regulation of IFN production. IRF3 is constitutively expressed and localizes exclusively in the cytoplasm as an inactive monomer in non-infected cells. Upon infection, IRF3 is phosphorylated, resulting in its dimerization and subsequent translocation to the nucleus, where it forms a complex with co-activator p300/CBP to induce IFN-β or IFN-α4 transcription (Haller et al., 2006).

Coronaviruses (CoV) are positive-stranded RNA viruses with a genome of approximately 30 kb. Murine hepatitis virus (MHV) is a group 2 CoV and is closely related to SARS-CoV, the causative agent of the severe acute respiratory syndrome (SARS) outbreak (Snijder et al., 2003). Previous studies have shown that infection of fibroblasts with MHV and SARS-CoV does not result in a significant induction of IFN production through intracellular detection by RNA helicases. However,

* Corresponding author. Fax: +31 715261667.
*E-mail address:* w.j.m.spaan@lumc.nl (W.J.M. Spaan).

0042-6822/$ - see front matter © 2007 Elsevier Inc. All rights reserved.
doi:10.1016/j.virol.2007.01.020

specialized cells that express TLRs are triggered to produce IFNs during CoV infection upon recognition of structural genes of the virus (reviewed in Versteeg and Spaan, in press). Together, these observations suggest that CoVs prevent IFN induction and the subsequent activation of antiviral genes. Recently, it has been shown that SARS-CoV non-structural protein 1 (nsp1) degrades mRNA, including IFN messengers (Kamitani et al., 2006) thereby impairing a proper innate immune response. Here we report that despite accumulation of dsRNA in infected cells, translocation of IRF3 to the nucleus does not occur in MHV- and SARS-CoV-infected cells. These data suggest that the absence of IRF3 activation is a general characteristic of group 2 coronaviruses. Furthermore we show that MHV and SARS-CoV do not actively block IRF3 activation via either RIG-I or MDA-5 as they are unable to inhibit IRF3 translocation upon Sendai virus infection or poly (I:C) transfection, respectively.

## Results

### *MHV is unable to prevent IFN induction by poly (I:C) and Sendai virus*

To directly compare transcription induction of immediate early IFNs by MHV and SARS-CoV, we stably transformed murine L cells with a plasmid coding for the SARS-CoV receptor, resulting in a cell line (L-ACE2) that supported infection with both MHV and SARS-CoV. SARS-CoV infected 100% of the cells and efficiently replicated in L-ACE2 cells, completing one round of replication in 12 h, similar to the widely used Vero-E6 cells (data not shown). In 12 h, virus titers in the medium increased to approximately $5 \times 10^8$ PFU/ml.

L-ACE2 cells were infected at MOI 10 with MHV to address IFN induction during infection. At 8 h p.i., intracellular RNA was isolated and IFN-α4 mRNA concentrations were determined by RT–qPCR. Despite efficient MHV progeny virus production (data not shown), MHV infection did not result in IFN-α4 (Fig. 1A) or IFN-β mRNA (data not shown) upregulation. Infection with different MHV strains (MHV-2, -JHM) in other cell lines (DBT, WBC264-9) did not trigger IFN transcription either (data not shown). As a control for IFN-α4 mRNA induction, mock-infected cells were transfected with poly (I:C). Poly (I:C) treatment resulted in an increase of IFN-α4 mRNA levels by approximately 280-fold (Fig. 1A), showing that these cells can be readily stimulated to initiate transcription of IFN genes. Next, MHV-infected cells were transfected with poly (I:C) to determine if MHV could actively prevent IFN induction through MDA-5-mediated IRF3 activation. Activation of IRF3 results in translocation of IRF3 to the nucleus which is a prerequisite for early IFN induction. In mock- and MHV-infected cells that were transfected with poly (I:C), a comparable fraction of the cells (85%) showed nuclear IRF3 translocation by IFA (Fig. 1B). Approximately 60–65% of those cells were infected with MHV, indicating that MHV cannot prevent IRF3 translocation to the nucleus and that it does not affect the ratio of cells displaying nuclear translocated IRF3. Moreover, poly (I:C) transfection stimulated IFN-α4 transcription to similar levels as in non-infected cells (Fig. 1A). Although more than 90% of all cells were MHV-infected after control transfection, the percentage of infected cells was reduced to approximately 60% after poly (I:C) treatment (Fig. 1B), indicating that although MHV infection can be established after poly (I:C) treatment, MHV is to some extent sensitive to IFN induction. Together, these data demonstrated that early IFNs were not induced by MHV infection and that MHV was unable to counteract IFN induction through MDA-5 by poly (I:C).

To determine whether MHV actively inhibited IRF3 signaling through RIG-I, L-ACE2 cells were infected with both MHV and SeV at an MOI of 5. Nuclear localization of IRF3 was analyzed by IFA in either MHV, SeV or MHV-SeV doubly infected cells. As shown in Fig. 1D, IRF3 was exclusively localized in the cytoplasm of cells that were infected with MHV only. This result is not due to impairment of IRF3 translocation in these particular cells since IRF3 translocated to the nuclei of SeV-infected cells, both in the absence and presence of MHV (Fig. 1D). Overall, 70% of the cells were infected with SeV and showed nuclear translocation of IRF3. Of those cells, 90% was also infected with MHV (Fig. 1D), indicating that MHV was unable to interfere with the nuclear translocation of IRF3 in cells that were infected with both MHV and SeV. The IFN-α4 mRNA levels in these doubly infected cells were comparable to cells infected with only SeV (Fig. 1C). Taken together, the data presented in Fig. 1 clearly demonstrated that MHV infection could not induce or prevent the RIG-I- or MDA-5-mediated immediate early IFN responses.

### *SARS-CoV is unable to prevent IFN induction by poly (I:C) and Sendai virus*

To confirm that SARS-CoV did not induce IFN in L-ACE2 cells and that the lack of IFN induction is a general feature of group 2 CoVs, we subsequently analyzed whether SARS-CoV was able to induce IFN production in L-ACE2 cells. Intracellular RNA was isolated and the induction of IFN-α4 was determined by RT–qPCR. Comparable to MHV-infected L-ACE2 cells, SARS-CoV-infected cells showed no increase in IFN-α4 (Figs. 2A/D) and IFN-β mRNA concentrations (data not shown) compared to mock-infected cells. Next, the ability of SARS-CoV to interfere with MDA-5 activated IFN responses when stimulated with poly (I:C) was investigated. L-ACE2 cells were infected with SARS-CoV at MOI 5 and subsequently transfected with poly (I:C). No IFN induction occurred during SARS-CoV infection. However, treatment with poly (I:C) stimulated IFN-α4 mRNA concentrations by 900-fold in both mock- as well as SARS-CoV-infected cells (Fig. 2A), suggesting that no interference by the virus occurred. A similar percentage of the cells was transfected with poly (I:C) as indicated by nuclear IRF3 localization in both mock- and SARS-CoV-infected samples (Fig. 2B), further illustrating the lack of interference with IFN induction by SARS-CoV. SARS-CoV replicative proteins were readily detected in one-third of the cells with nuclear IRF3, further indicating that SARS-CoV did not significantly prevent IRF3 translocation (Fig. 2B).

Subsequently, L-ACE2 cells were infected with both SeV and SARS-CoV at an MOI of 1 to establish whether SARS-CoV could actively inhibit IFN mRNA synthesis through RIG-I. At 12 h p.i., RNA was isolated. As determined by RT–qPCR, SeV infection of L-ACE2 cells resulted in an 80-fold IFN-α4 mRNA increase at 12 h p.i. compared to mock-infected cells

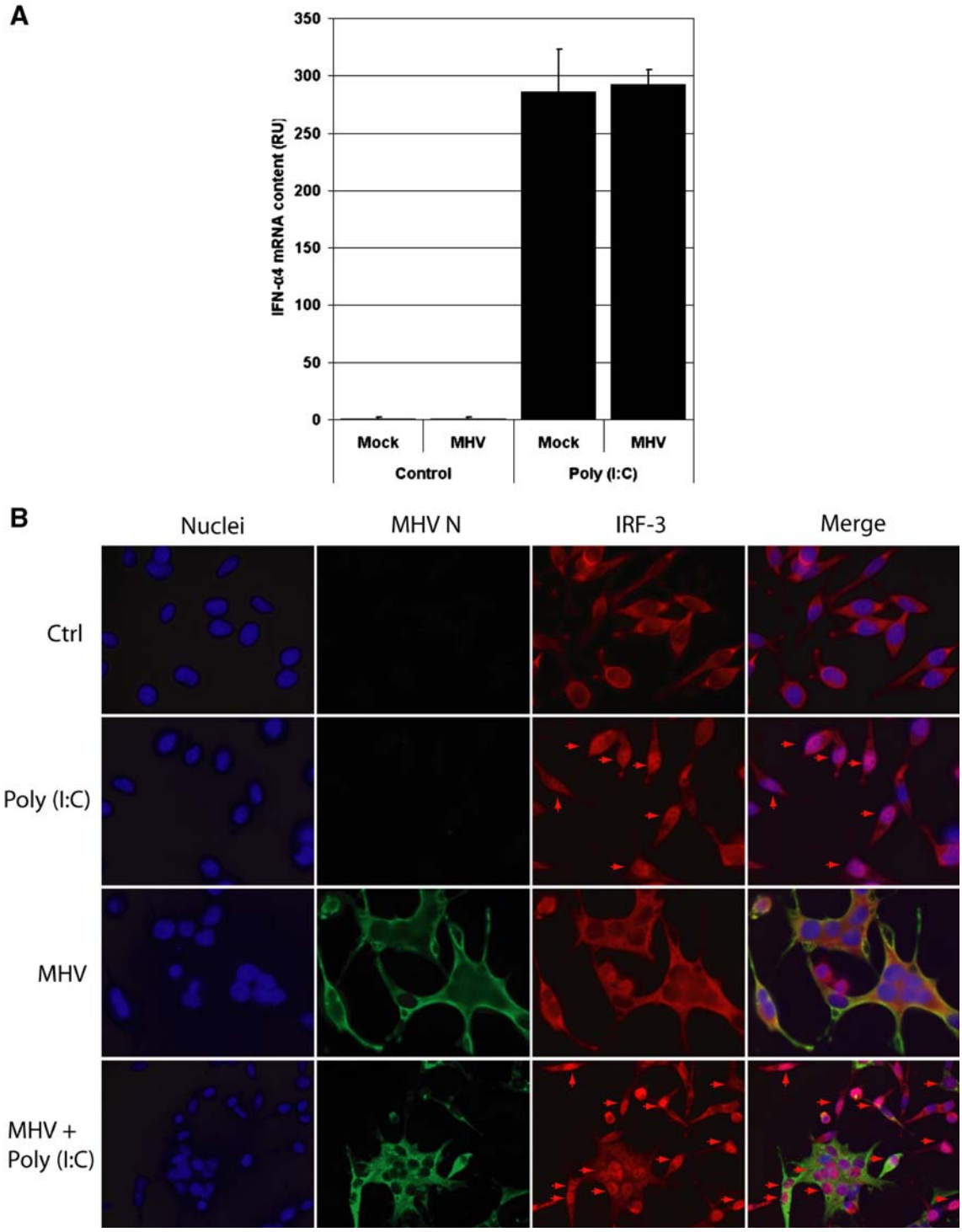


Fig. 1. L-ACE2 cells were infected with MHV at MOI 10. At 1 h p.i., cells were transfected with 4 μg poly (I:C). At 8 h p.i. total RNA was isolated and reverse transcribed using random hexamers. (A) IFN-α4 mRNA concentration was determined using specific RT–qPCR and (B) endogenous IRF3 localization and MHV nucleocapsid protein were detected in IFA with specific poly- and monoclonal antibodies, respectively. Nuclear IRF3 is indicated with arrows. Subsequently, L-ACE2 cells were seeded on coverslips in 35-mm wells and infected with SeV for 30 min. Next, cells were infected with MHV at MOI 5. At 8.5 h p.i. cells on coverslips were fixed in 3% paraformaldehyde. From the remainder of the cells, total RNA was isolated and reverse transcribed using random hexamers. (C) IFN-α4 mRNA concentration was determined using specific RT–qPCR and (D) endogenous IRF3 and MHV nucleocapsid protein were detected in IFA with specific poly- and monoclonal antibodies, respectively. Nuclear IRF3 is indicated with arrows.

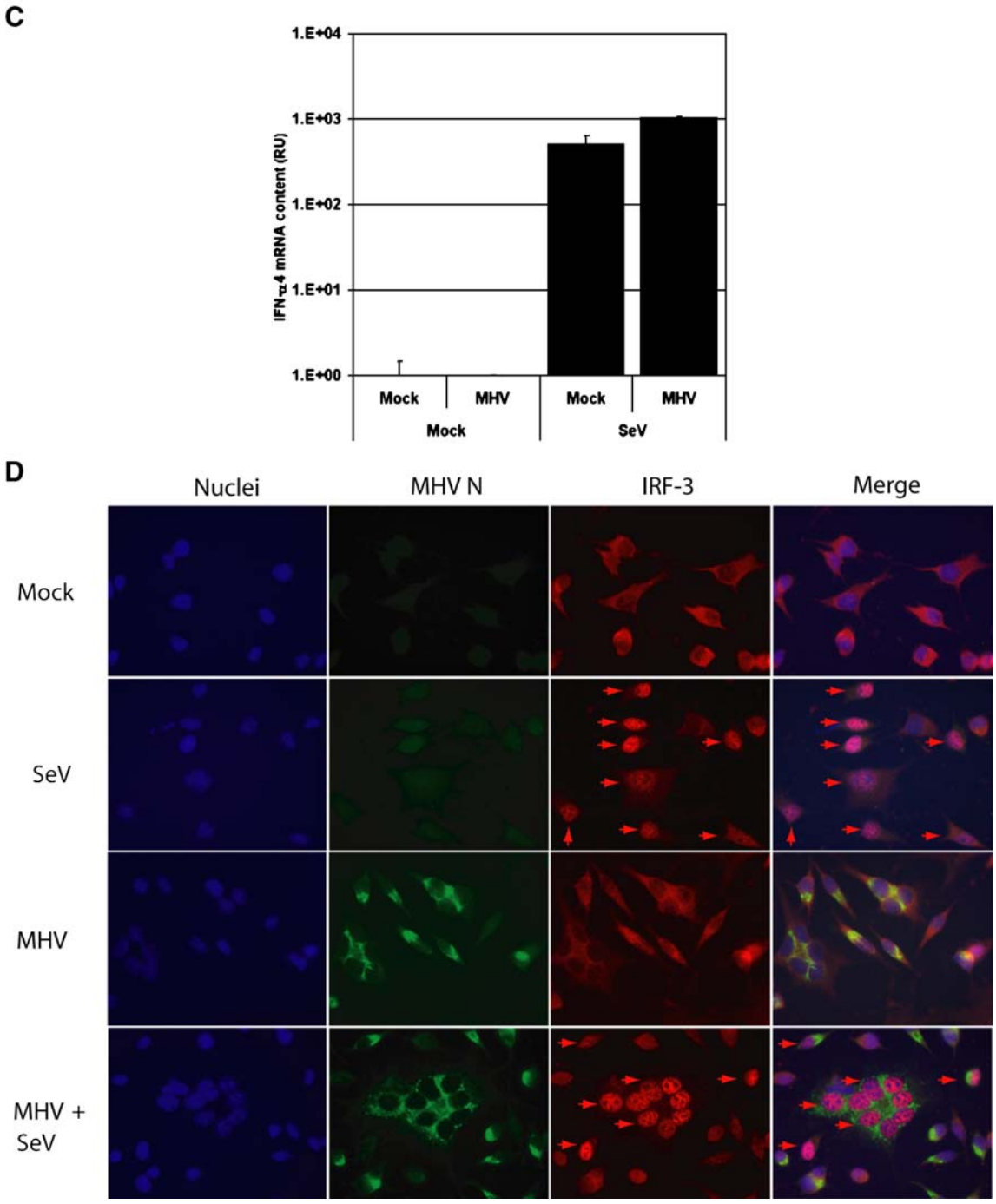


Fig. 1 (*continued*).

(Fig. 2D). SARS-CoV infection did not reduce IFN-α4 mRNA induction in L-ACE2 cells by SeV (Fig. 2D) compared to SeV infection only. IRF3 translocation to the nucleus was determined by IFA, to establish whether the lack of IFN-α4 induction in SARS-CoV-infected cells resulted from absence of IRF3 translocation to the nucleus. In mock- and SARS-CoV-infected cells IRF3 resided in the cytoplasm, while in SeV or SARS-CoV and SeV doubly infected cells IRF3 was translocated to the nucleus (Fig. 2C). Approximately 65% of those cells were doubly infected (Fig. 2C), indicating that SARS-CoV does not interfere with nuclear IRF3 localization in SeV-infected cells and does not influence the percentage of cells with nuclear IRF3.

*dsRNA accumulates in SARS-CoV- and MHV-infected cells*

It has been suggested that low levels of dsRNA in CoV-infected cells could be the reason for lack of IFN induction, rather than interference with components of the IFN induction pathways (Sawicki and Sawicki, 2005). To determine the formation of dsRNA during viral replication, L-ACE2 cells infected with either MHV or SARS-CoV were fixed at 8 and

12 h p.i.. The presence of dsRNA in MHV- or SARS-CoV-infected cells was determined by IFA using a dsRNA-specific antibody. No signal was observed in mock-infected cells, while dsRNA was detected in both MHV- and SARS-CoV-infected cells (Fig. 3), indicating the production of significant amounts of dsRNA during CoV infection.

## Discussion

The results reported here demonstrated that infection with MHV and SARS-CoV does not induce immediate early IFNs in fibroblast-like cells. We conclude that viral RNA in CoV-infected cells is not recognized by cellular sensors based on the

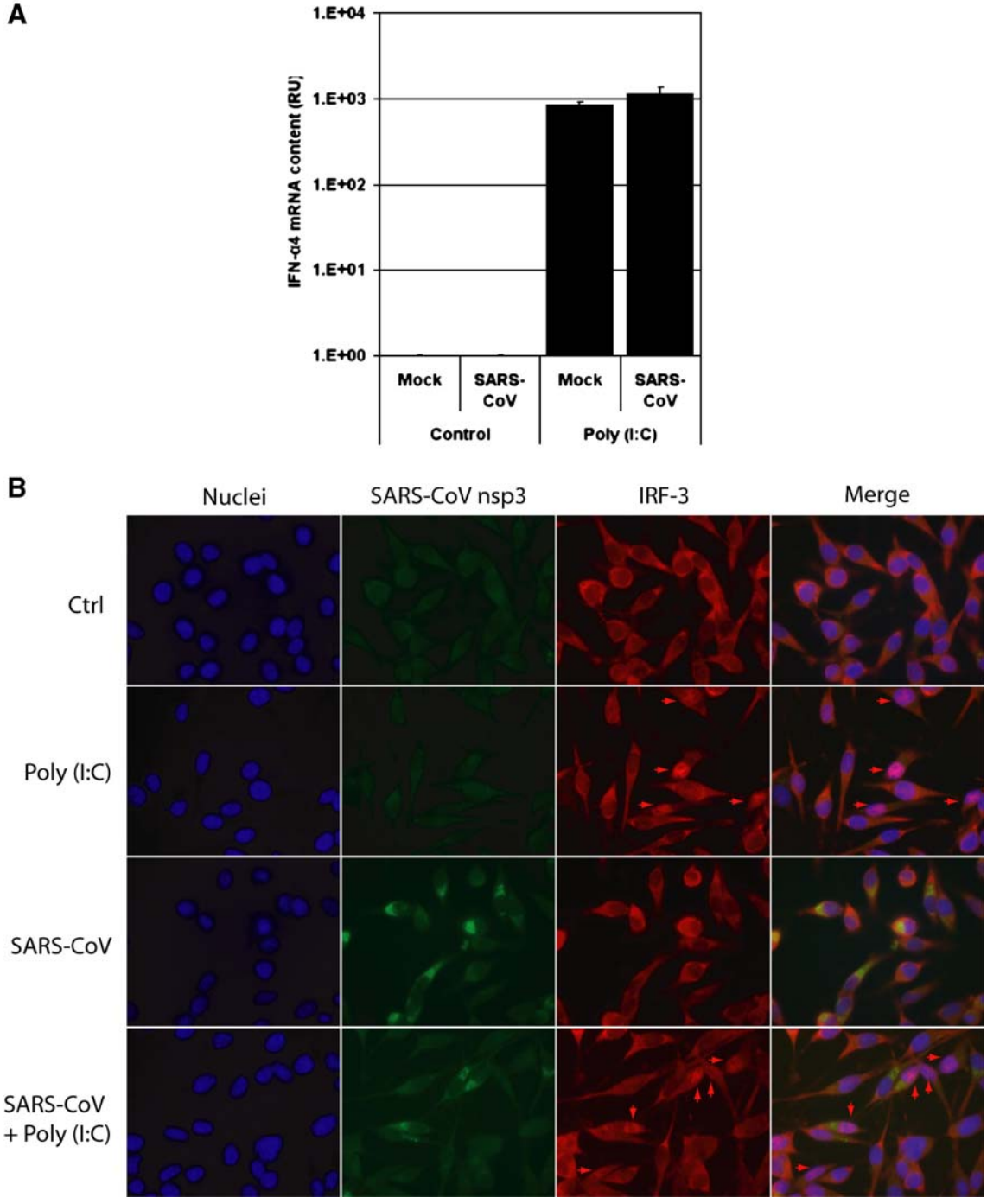


Fig. 2. L-ACE2 cells were infected with SARS-CoV at MOI 5. At 1 h p.i., cells were transfected with 4 μg poly (I:C). At 8 h p.i. total RNA was isolated and reverse transcribed using random hexamers. (A) IFN-α4 mRNA concentration was determined using specific RT–qPCR and (B) endogenous IRF3 localization and SARS-CoV nsp3 protein were detected in IFA with specific antibodies. Nuclear IRF3 is indicated with arrows. Subsequently, L-ACE2 cells were infected with SeV or SARS-CoV at MOI 1. At 12 h p.i. total RNA was isolated and reverse transcribed using random hexamers and coverslips were fixed in 3% paraformaldehyde. (C) IRF3 localization and SARS-CoV nsp3 protein were analyzed by immunofluorescence. Nuclear IRF3 is indicated with arrows. (D) IFN-α4 mRNA concentration was determined using specific RT–qPCR.

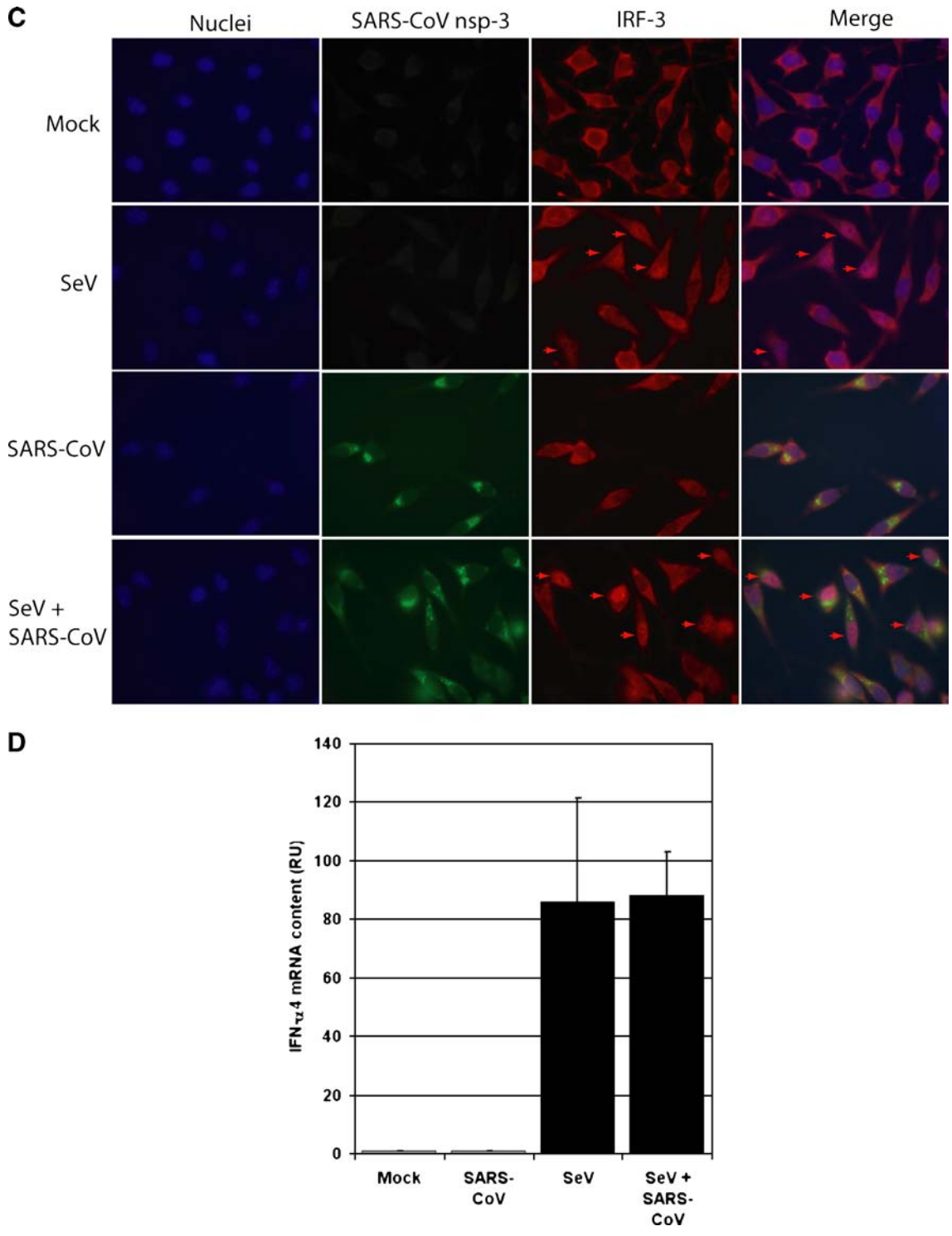


Fig. 2 (*continued*).

following observations: (i) nuclear IRF3 translocation or IFN mRNA transcription was not triggered during MHV and SARS-CoV infection despite the presence of dsRNA and (ii) MHV and SARS-CoV could not interfere with nuclear IRF3 translocation and IFN induction through RIG-I by SeV or through MDA-5 by poly (I:C). Viruses have evolved multiple mechanisms to prevent or inactivate IFN-mediated antiviral immunity at the level of IRF3 activation (Haller et al., 2006). For example, influenza virus NS1 and E3L from poxviruses are dsRNA binding proteins that prevent IRF3 activation by sequestering viral RNA and thereby circumvent recognition by RIG-I and MDA-5. The V protein of several paramyxoviruses interacts directly with MDA-5 and prevents as such IRF3 activation and subsequent IFN induction. The hepatitis C virus protease NS3/4A cleaves the adaptor molecule VISA. The P protein of Borna disease virus (BDV) inhibits IRF3 phosphorylation by

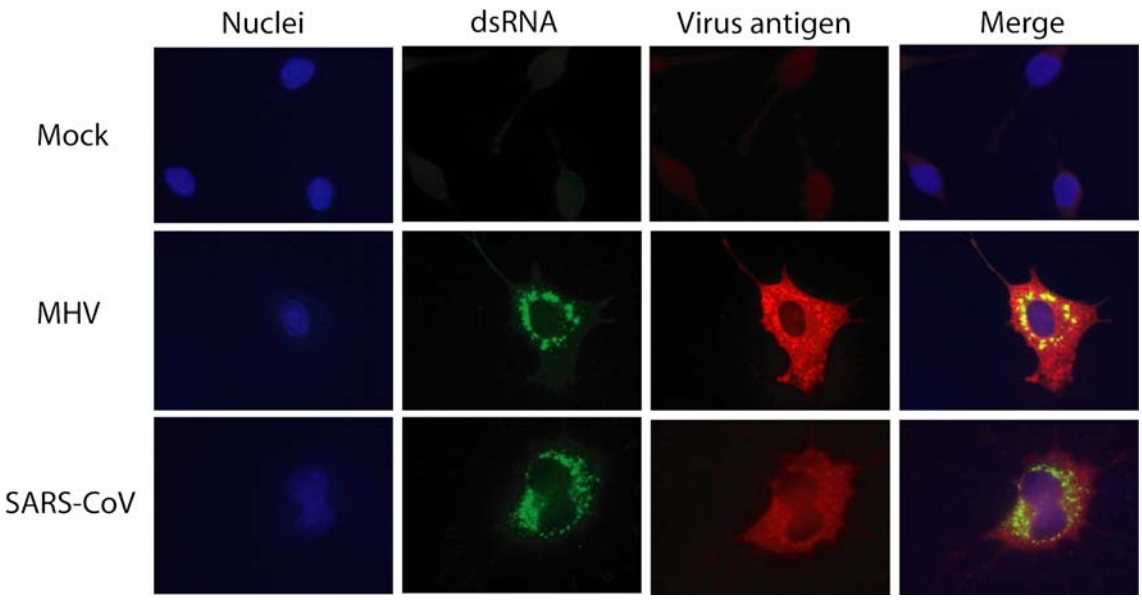


Fig. 3. L-ACE2 cells were infected with MHV or SARS-CoV at MOI 10 and 1, respectively. At 8 h after MHV infection or 12 h after SARS-CoV infection, cells were fixed in 3% paraformaldehyde. MHV and SARS-CoV were detected in IFA using specific polyclonal antibodies raised against MHV virions and SARS-CoV N protein, respectively. dsRNA was detected in IFA with specific monoclonal antibodies.

averting proper functioning of kinase TBK1 (Haller et al., 2006). Importantly, hepatitis A virus infection has been reported to interfere with IRF3 translocation and IFN production induced by poly (I:C) and an exogenous virus, very similar to the approach described in this manuscript (Fensterl et al., 2005). These viruses all actively interfere with the IFN induction pathway, rather than preventing its initial activation. However, our data indicate that MHV, SARS-CoV and possibly other group 2 CoVs have devised a yet undescribed mechanism where viral RNA is protected from the host cell's sensory molecules.

MHV replication requires ongoing viral protein synthesis (Sawicki and Sawicki, 2005). In contrast to e.g. alphaviruses, MHV replication complexes are unstable and replication is marked by high turn-over of minus-strand RNA, whereas plus-strand RNA is relatively stable (Sawicki and Sawicki, 2005). The unstable nature of the minus-strand RNA has been suggested to prevent the formation of stable dsRNA replicative intermediates/forms and subsequent triggering of the IFN response through MDA-5 (Sawicki and Sawicki, 2005). Immunofluorescence labeling with a dsRNA-specific antibody (Fig. 3) strongly suggests that significant amounts of dsRNA are formed during CoV infection and that rapid turn-over of minus-strand RNA is unlikely to explain the lack of IFN induction. Since substantial amounts of dsRNA are present in infected cells (Fig. 3), our data suggest that an additional form of protection of the dsRNA underlies the lack of IRF3 activation and IFN RNA synthesis (Figs. 1 and 2). In comparison to MDA-5, RIG-I-mediated IFN induction depends on 5′-triphosphates rather than dsRNA (Hornung et al., 2006; Pichlmair et al., 2006). dsRNA without 5′-triphosphates like poly (I:C), picornavirus RNA which contains VPg at the 5′-end or capped RNAs do not trigger IFN responses through RIG-I, but utilize MDA-5 (Kato et al., 2006). Coronavirus RNA is capped during replication by which RIG-I induction could be prevented (Lai et al., 1982). Since viral RNA synthesis occurs in the cytoplasm and host cell RNA modifications such as capping occur in the nucleus, many viruses have devised strategies to provide their own RNA modification machinery. All group 2 coronaviruses encode five homologs of cellular enzymes involved in RNA processing (Snijder et al., 2003). One of them is a 2′-*O*-methyltransferase which could play a role in capping of the viral RNA.

The nature of the replication complex could create a compartment that prevents replicating RNA from being detected by the host cell. CoV replication complexes are associated with host cell membranes which could create such an environment. Although this is a general feature of all other positive-stranded RNA viruses, association with double membrane vesicles (DMV) has exclusively been reported for corona- and picornaviruses so far (Gosert et al., 2002; Snijder et al., 2006). These DMVs could facilitate replication by compartmentalizing replication factors and providing structural support for membrane anchoring. Furthermore, DMVs could form a protective microenvironment that prevents viral RNA from being detected by host cell sensors. The fact that picornaviruses have also devised other mechanisms to actively interfere with correct induction and functioning of the IFN response (Haller et al., 2006) suggests that the formation of DMVs is apparently not sufficient to prevent IFN induction per se. Current knowledge on the similarities of the DMVs of these two virus families is insufficient to establish whether differential organization of CoV and picornavirus DMVs could explain these different properties. A recent report by Kato and co-workers suggested that viruses within the same families trigger IFN responses through the same pathway (Kato et al., 2006). We demonstrated that MHV does not interfere with the RIG-I or MDA-5 pathway. However, we cannot rule out that CoVs induce IFN responses through other cellular molecules than RIG-I or MDA-5 at this point. Although CoVs may express proteins that affect IFN

induction when expressed separately, here we demonstrate that in the context of virus infection, CoVs do not significantly interfere directly with IRF3 translocation or IFN transcription. However, Spiegel and co-workers have reported nuclear IRF-3 localization during SARS-CoV infection (Spiegel et al., 2005). It is currently unclear what underlies the discrepancy with our data. Their infections were performed using another SARS-CoV strain (FFM1) and different cells (a selected 293-cell clone) what may explain the differences. Similar results to ours showing the inability of MHV-A59 to interfere with MDA-5- or RIG-I-mediated IFN induction were recently published (Zhou and Perlman, 2007). The results presented in our work confirm and support those findings. The new data on SARS-CoV provide evidence that all group 2 CoVs may employ a similar mechanism to prevent IFN induction.

Infection of fibroblasts with MHV and SARS-CoV does not result in a significant IFN production. However, specialized cells that express TLRs are triggered to produce IFN during CoV infection (reviewed in Versteeg and Spaan, 2006). Furthermore, plasmatoid dendritic cells (pDC) are the predominant cells to produce systemic IFN during MHV infection in vivo (Cervantes-Barragan et al., 2007). The experiments described in this paper were all performed in non-specialized (immune) cells. Although the significance of the absence of IFN induction in these cells remains to be established, we hypothesize that it could give the virus a temporal advantage early in in vivo infections before it disseminates through the body.

## Materials and methods

### *Cells and viruses*

Mouse L cells and Sac$^-$ cells were cultured and infected with MHV as described before (Jacobs et al., 1981). L cells stably expressing the SARS-CoV receptor angiotensin converting enzyme 2 (L-ACE2) were constructed by transformation of L cells with plasmid pcDNA3/FLACE2 (Broer et al., 2006). Full details will be published elsewhere. L-ACE2 cells were maintained as regular L cells, with the only exception that the medium was supplemented with 500 μg/ml G418. Strain A59 of MHV was obtained from ATCC. SARS-CoV strain Frankfurt 1 was grown on Vero-E6 cells and all work with infectious SARS-CoV was performed as described (Snijder et al., 2006). MOI 1–10 was used for coronavirus infections throughout this study. MHV and SARS-CoV titers were determined by plaque assays on L cells and L-ACE2 cells, respectively. Recombinant Sendai virus H4 (SeV-H4) (Cadd et al., 1996) was kindly provided by D. Kolakofsky. SeV-H4 infections were carried out in complete medium for 30–45 min at 37 °C after which complete medium was added to the inoculum.

### *RNA isolation and quantitative RT–PCR*

Total RNA was isolated from cells at the indicated times p.i. using TRIzol reagent (Invitrogen). RNA was treated with 2 units of DNaseI (Invitrogen) at 37 °C for 30 min to remove potential DNA contamination. Quantitative RT–PCR (RT–qPCR) was performed as described previously (Versteeg et al., 2006). Primer sequences are available on request.

### *IFN induction by poly (I:C)*

L-ACE2 cells were washed with phosphate-buffered saline (PBS) and infected with MHV or SARS-CoV in DMEM containing 3% FCS. At 1 h p.i., cells were washed with PBS and transfected with 4 μg poly (I:C) (Sigma) using Lipofectamine 2000 (Invitrogen) as recommended by the manufacturer. Subsequently, cells were incubated for another 7 h at 37 °C.

### *Antisera and immunofluorescence assay*

Cells were seeded on glass coverslips in 35-mm wells, infected and subsequently transfected as described above. Coverslips were removed at set intervals, fixed in 3% paraformaldehyde and further processed for immunofluorescence assay as described previously (Snijder et al., 2006). Cells were incubated with either 1:1000 diluted rabbit k134 serum raised against MHV particles (Rottier et al., 1981), 1:400 diluted anti-IRF3 (Zymed), 1:400 diluted 5B188.2 anti-MHV N (Talbot et al., 1984), 1:500 diluted anti-SARS-CoV nsp-3 directly coupled to Alexa Fluor 488 dye (Snijder et al., 2006) or 1:400 diluted anti-dsRNA antibody (Weber et al., 2006). Samples were examined with a Zeiss Axioskop 2 fluorescence microscope. Monoclonal antibodies were detected using Alexa Fluor 488-conjugated goat anti-mouse secondary antibodies (Invitrogen). Polyclonal antibodies were detected with Cy3-conjugated donkey anti-rabbit secondary antibodies (Invitrogen). Nuclei were labeled by DNA staining using Hoechst 33342 dye.

## Acknowledgments

We thank Jeroen Corver, Jessika Zevenhoven-Dobbe and Eric Snijder for their significant contribution in construction and characterization of the L-ACE2 cell line.

## References

Broer, R., Boson, B., Spaan, W., Cosset, F.L., Corver, J., 2006. Important role for the transmembrane domain of severe acute respiratory syndrome coronavirus spike protein during entry. J. Virol. 80, 1302–1310.

Cadd, T., Garcin, D., Tapparel, C., Itoh, M., Homma, M., Roux, L., Curran, J., Kolakofsky, D., 1996. The Sendai paramyxovirus accessory C proteins inhibit viral genome amplification in a promoter-specific fashion. J. Virol. 70, 5067–5074.

Cervantes-Barragan, L., Zust, R., Weber, F., Spiegel, M., Lang, K.S., Akira, S., Thiel, V., Ludewig, B., 2007. Control of coronavirus infection through plasmacytoid dendritic-cell-derived type I interferon. Blood 109, 1131–1137.

Fensterl, V., Grotheer, D., Berk, I., Schlemminger, S., Vallbracht, A., Dotzauer, A., 2005. Hepatitis A virus suppresses RIG-I-mediated IRF-3 activation to block induction of beta interferon. J. Virol. 79, 10968–10977.

Gosert, R., Kanjanahaluethai, A., Egger, D., Bienz, K., Baker, S.C., 2002. RNA replication of mouse hepatitis virus takes place at double-membrane vesicles. J. Virol. 76, 3697–3708.

Haller, O., Kochs, G., Weber, F., 2006. The interferon response circuit: induction and suppression by pathogenic viruses. Virology 344, 119–130.

Hornung, V., Ellegast, J., Kim, S., Brzozka, K., Jung, A., Kato, H., Poeck, H., Akira, S., Conzelmann, K.K., Schlee, M., Endres, S., Hartmann, G., 2006. 5′-Triphosphate RNA is the ligand for RIG-I. Science 314, 994–997.

Jacobs, L., Spaan, W.J., Horzinek, M.C., Van der Zeijst, B.A., 1981. Synthesis of subgenomic mRNAs of mouse hepatitis virus is initiated independently: evidence from UV transcription mapping. J. Virol. 39, 401–406.

Kamitani, W., Narayanan, K., Huang, C., Lokugamage, K., Ikegami, T., Ito, N., Kubo, H., Makino, S., 2006. Severe acute respiratory syndrome coronavirus nsp1 protein suppresses host gene expression by promoting host mRNA degradation. Proc. Natl. Acad. Sci. U.S.A. 103, 12885–12890.

Kato, H., Takeuchi, O., Sato, S., Yoneyama, M., Yamamoto, M., Matsui, K., Uematsu, S., Jung, A., Kawai, T., Ishii, K.J., Yamaguchi, O., Otsu, K., Tsujimura, T., Koh, C.S., Reis e Sousa, C., Matsuura, Y., Fujita, T., Akira, S., 2006. Differential roles of MDA5 and RIG-I helicases in the recognition of RNA viruses. Nature 441, 101–105.

Lai, M.M., Patton, C.D., Stohlman, S.A., 1982. Further characterization of mRNAs of mouse hepatitis virus: presence of common 5′-end nucleotides. J. Virol. 41, 557–565.

Pichlmair, A., Schulz, O., Tan, C.P., Naslund, T.I., Liljestrom, P., Weber, F., Reis e Sausa, 2006. RIG-I-mediated antiviral responses to single-stranded RNA bearing 5′-phosphates. Science 314, 997–1001.

Rottier, P.J., Spaan, W.J., Horzinek, M.C., Van der Zeijst, B.A., 1981. Translation of three mouse hepatitis virus strain A59 subgenomic RNAs in *Xenopus laevis* oocytes. J. Virol. 38, 20–26.

Sawicki, S.G., Sawicki, D.L., 2005. Coronavirus transcription: a perspective. Curr. Top. Microbiol. Immunol. 287, 31–55.

Snijder, E.J., Bredenbeek, P.J., Dobbe, J.C., Thiel, V., Ziebuhr, J., Poon, L.L., Guan, Y., Rozanov, M., Spaan, W.J., Gorbalenya, A.E., 2003. Unique and conserved features of genome and proteome of SARS-coronavirus, an early split-off from the coronavirus group 2 lineage. J. Mol. Biol. 331, 991–1004.

Snijder, E.J., van der, M.Y., Zevenhoven-Dobbe, J., Onderwater, J.J., van der, M.J., Koerten, H.K., Mommaas, A.M., 2006. Ultrastructure and origin of membrane vesicles associated with the severe acute respiratory syndrome coronavirus replication complex. J. Virol. 80, 5927–5940.

Spiegel, M., Pichlmair, A., Martinez-Sobrido, L., Cros, J., Garcia-Sastre, A., Haller, O., Weber, F., 2005. Inhibition of beta interferon induction by severe acute respiratory syndrome coronavirus suggests a two-step model for activation of interferon regulatory factor 3. J. Virol. 79, 2079–2086.

Talbot, P.J., Knobler, R.L., Buchmeier, M.J., 1984. Western and dot immunoblotting analysis of viral antigens and antibodies: application to murine hepatitis virus. J. Immunol. Methods 73, 177–188.

Versteeg, G.A., Spaan, W.J., in press. Host cell responses to coronavirus infections. The Nidoviruses (ASM Press).

Versteeg, G.A., Slobodskaya, O., Spaan, W.J., 2006. Transcriptional profiling of acute cytopathic murine hepatitis virus infection in fibroblast-like cells. J. Gen. Virol. 87, 1961–1975.

Weber, F., Wagner, V., Rasmussen, S.B., Hartmann, R., Paludan, S.R., 2006. Double-stranded RNA is produced by positive-strand RNA viruses and DNA viruses but not in detectable amounts by negative-strand RNA viruses. J. Virol. 80, 5059–5064.

Zhou, H., Perlman, S., 2007. Mouse hepatitis virus does not induce beta interferon synthesis and does not inhibit its induction by double-stranded RNA. J. Virol. 81, 568–574.